Title: Range expansion is both slower and less predictable across a spatial gradient in temperature

Authors: Takuji Usui[1], Amy L. Angert[1,2]

Author affiliations:
[1]Department of Botany, University of British Columbia, Vancouver, British Columbia, V6T 1Z4, Canada (usuitakuji@gmail.com)
[2]Department of Zoology, University of British Columbia, Vancouver, British Columbia, V6T 1Z4, Canada (angert@mail.ubc.ca)

Corresponding author: Takuji Usui (Department of Botany, University of British Columbia, 2122 Main Mall, Vancouver, BC, V6T 1Z4, Canada; email: usuitakuji@gmail.com)

Running title: Range expansion across abiotic gradients

Keywords: biological invasion; demography; dispersal; eco-evolutionary dynamics; environmental gradient; experimental evolution; priority effects; range limit; variability

Article type: Letter
Word counts: Abstract (150), Main text (4989)
Number of references: 52
Number of figures: 4

Statement of authorship: TU conceived of this study with guidance from ALA. TU collected the data. TU analysed the data, developed the figures, and wrote the first draft of the manuscript with feedback from ALA. TU and ALA contributed to edits in preparation for manuscript submission.

Data accessibility statement: Data and R codes used for analyses are available on Zenodo:

## ABSTRACT

Rapid evolution in colonizing populations can alter our ability to predict future range expansions. Recent studies suggest that how evolution influences the predictability of range expansion speed depends on the balance of genetic drift and selection at the range front, with factors increasing selection proposed to produce greater consistency, and hence increased predictability, in range expansion speed. Here, we test whether selection from environmental gradients across space produces more predictable range expansion speeds, using the experimental evolution of replicate, duckweed populations colonizing landscapes with and without a temperature gradient. While range expansion across a temperature gradient was slower, with range-front populations displaying higher population densities and genetic signatures consistent with greater selection, we found that range expansion speed was more variable and less predictable across replicate populations. Our results therefore challenge current theory, highlighting that selection and spatial priority effects could together govern the predictability of range expansion speeds.

## INTRODUCTION

Predicting the movement of species ranges is a fundamental goal of ecology and is of increasing importance as biological invasions and climate change accelerate range expansion (Chen et al. 2011; Iseli et al. 2023; Nadeau & Urban 2019). Classic work on the ecological dynamics of range expansion has demonstrated that higher values of two key life-history traits – dispersal and reproductive output – increase the speed of range expansion (Kot et al. 1996; Skellam 1951). More recent work incorporating rapid evolution has shown that not only can dispersal and reproduction evolve to increase the average speed of range expansion, but that additionally, evolution can directly influence the amount of variability in the speed of population spread

54 across replicate, range-expanding populations (Miller et al. 2020; Ochocki & Miller 2017;
55 Williams et al. 2016; Wiliams et al. 2019). However, when and in what direction evolution
56 modifies the variability, and hence predictability, of range expansion remains unclear.
57
58 On one hand, eco-evolutionary studies of range expansion predict that evolution should increase
59 variability in range expansion speed across replicate populations. Specifically, serial founding
60 events during range expansion can result in the fixation of maladaptive alleles at the range front
61 and consequent reduction in fitness ('expansion load') through a spatial analogue of genetic drift
62 ('gene surfing') (Excoffier et al. 2009; Klopfstein et al. 2006; Perrier et al. 2020). Gene surfing
63 in small, range-expanding populations leads to the fixation of random amounts of expansion load
64 across replicate populations, thus generating variability in range expansion speed (Miller et al.
65 2020; Phillips 2015; Williams et al. 2019). The implication then, is that any single realisation of
66 range expansion in nature is drawn from a distribution of possible outcomes, making predictions
67 of range expansion more difficult.
68
69 In contrast, some recent experimental work testing the predictability of range expansions shows
70 that evolution can also reduce variance in range expansion speed (Miller et al. 2020; Williams et
71 al. 2019). This is predicted to occur when directional selection (e.g., for traits conferring greater
72 dispersal or environmental tolerance; Chuang & Peterson 2016; Freedman et al. 2020; Lancaster
73 et al. 2015) reduces trait variance at the range front, hence increasing consistency in the average
74 speed of range expansion (Phillips 2015; Williams et al. 2019). Overall, how evolution modifies
75 the variability in range expansion speed may therefore depend on the relative strength of gene

surfing and selection in range-front populations, and the factors that tip this balance one way or another (Miller et al. 2020; Urquhart-Cronish et al. 2022; Williams et al. 2019).

One key factor that could tip this balance between the variance-generating and variance-reducing effects of evolution is environmental variation in space. Specifically, species' ranges in nature exist across broad-scale spatial abiotic gradients. Importantly, changing abiotic conditions across space could lead to slower range expansion due to the need for populations to adapt to the underlying abiotic gradient. This initial maladaptation at the range front can allow more time for individuals to arrive from the range core, consequently increasing population size and genetic variation at the range front over time (Fronhofer et al. 2017; Gilbert et al. 2017). In these 'steeper' range boundaries, directional selection favouring traits that confer tolerance to changing abiotic conditions could weaken gene surfing and its genetic and demographic consequences (Gilbert et al. 2017; Williams et al. 2019). Thus, selection from underlying abiotic gradients in space could make the speed of range expansion among replicate populations less variable and more predictable. Although there is a need to incorporate realistic sources of environmental variation, experimentally testing how selection from abiotic gradients in space modifies the predictability of replicate range expansions in nature remains difficult (Miller et al. 2020).

Experimental range expansions in "miniaturised" landscapes (Larsen & Hargreaves 2020; Lustenhower et al. 2023) can provide a powerful bridge between theory and range expansion in natural landscapes. First, these landscapes differ from traditional microcosms in that replicate populations can disperse naturally across linear landscapes, such that realistic genetic and demographic spatial structure arises during range expansions. Second, through replicated

99 landscapes we can track a distribution of ecological and evolutionary outcomes in colonising
100 populations. This allows experimental insights into the factors that contribute to variability in
101 range expansion that would not be possible without replication. Third, through experimental
102 evolution we can track the eco-evolutionary dynamics of range expansion unfolding over
103 multiple generations in real time, while field studies have mostly been retrospective, inferring
104 past demographic and evolutionary processes based on current spatial patterns. Despite the
105 increasing utility of these landscapes (Larsen & Hargreaves 2020), we still require experiments
106 that test the dynamics of range expansion across landscapes that incorporate selection from
107 spatial environmental variation.
108
109 Here, we use experimental populations of duckweeds in the *Lemna* species complex to
110 experimentally test how selection from spatial abiotic gradients modifies the predictability (i.e.,
111 among-replicate variability) of range expansion speed. Using replicate landscapes with and
112 without a temperature gradient in space, we predicted that: (i) range expansion speed should be
113 more predictable (i.e., less variable among replicates) when populations move across landscapes
114 with a spatial temperature gradient than without. We predicted that this would occur as: (ii) range
115 expansion across temperature gradients would be on average slower, resulting in higher
116 population densities and steeper range boundaries. Consequently, we predicted that there should
117 be stronger signatures of selection over genetic drift in populations expanding across temperature
118 gradients. If selection was stronger in populations expanding across temperature gradients in
119 space, then we predict: (iii) less among-replicate variability in genotypic composition for
120 gradient than uniform landscapes; and (iv) directional selection for traits relevant to thermal
121 tolerance in these populations.

## MATERIALS & METHODS

### *Lemna* species collection and culturing

Duckweeds in the genus *Lemna* (family Araceae) are small, freshwater angiosperms with a rapid generation time of 2–5 days under ideal conditions (Landolt 1986). Although sexual reproduction occurs sporadically in nature, reproduction during experiments occurs exclusively through the clonal budding of daughter fronds (Docauer 1983; Landolt 1986). Multiple fronds can stay connected via a stipule to form rafts of ~3-5 fronds until the stipule breaks and daughter fronds disperse. We sampled 20 unique *Lemna* accessions from 20 sites around the Pacific Northwest region of North America (Table S1). Upon sampling, we immersed fronds in a dilute bleach solution (10% v:v) to create axenic plants of each accession. We maintained each of our 20 accessions in 250 mL erlenmeyer flasks with 100 mL of artificial pond media (Appenroth et al. 1996), inside a temperature-controlled laboratory (20°C) and under full-spectrum LED lighting (SunBlaster 6400K; 16:8 hour light:dark cycle). To obtain sufficient numbers of individuals for the experiment, we grew out each accession for 4 weeks inside 20 L buckets at the UBC Botany greenhouse, with 17 L of water, 4 L of autoclaved potting soil (MiracleGro Potting Mix), 1.32 mM of $KNO_3$, 0.16 mM of $Ca(NO_3)_2$, and 0.02 mM of $KH_2PO_4$ as fertilisers.

Subsequent barcoding and microsatellite genotyping of each accession detected that our accessions were composed of 10 unique genotypes of the common duckweed *Lemna minor* and one genotype of the cryptic species *Lemna turionifera* (Appendix S1; Tables S1-S3). These two species are part of the *Lemna* species complex, consisting of *L. minor*, *L. turionifera*, and *L. japonica*, with the latter classified as a hybrid between the two former species (Braglia et al.

145 2021a; Braglia et al. 2021b; Volkova et al. 2023). These species are morphologically and
146 genetically cryptic, with some previous studies considering *L. turionifera* to be an ecotype of *L.*
147 *minor* (Docauer 1983). We similarly found that these two species had comparable characteristics
148 in trait space (Fig. S1). For our experiment, we therefore describe evolution in populations as
149 occurring through the sorting of unique genotypes within the *Lemna* species complex.
150

151 **Experimental landscapes and temperature treatment**

152 We set up 50 experimental landscapes across five benches inside the greenhouse, with each
153 landscape constructed from aluminium gutters (150 cm x 12.5 cm; L x W) and filled with 13.5 L
154 of water and 2.5 L of potting soil. To ensure nutrients and water-levels did not deplete over time,
155 we added 0.13 mM of $KNO_3$, 0.02 mM of $Ca(NO_3)_2$, and 0.002 mM of $KH_2PO_4$ every 4 days to
156 each landscape, and continuously regulated water-levels using a float-valve connected to a sump
157 pump. We connected drip emitters to the sump pump so that water refilling occurred slowly and
158 did not disrupt the spatial structure of populations. We set up a temperature treatment (Fig. 1a)
159 such that range expansion occurred across landscapes with a spatial gradient in temperature
160 ("gradient landscapes" hereafter; $N = 25$) or with spatially uniform temperatures ("uniform
161 landscapes" hereafter; $N = 25$). The position of gradient and uniform landscapes was randomised
162 within each bench. To establish a temperature gradient, we used a submersible heater (150W JBJ
163 aquarium heaters) set to 37°C and placed at one end of each gradient landscape. To maintain
164 uniform temperatures, we placed two heaters set to 24°C at both ends of each uniform landscape.
165 These set temperatures were chosen as they are close to the critical thermal maxima ($T_{max}$) and
166 thermal optima ($T_{opt}$), respectively, of the *Lemna* genotypes used (Fig. S1). We monitored water
167 temperatures using three underwater temperature loggers (HOBO pendants) placed at equal

168 spacing within each landscape. For gradient and uniform landscapes, the imposed temperature
169 treatment resulted in increasing or uniform temperatures across space, respectively (Fig. 1b).
170 Although our initial aim for gradient landscapes was to set up a stress gradient such that
171 populations experienced increasing heat stress as they dispersed, we note that: (i) average
172 temperatures at the experimental range limit of gradient landscapes were still relatively benign
173 (31.6°C; SD = 1.9°C; Fig. 1b); and (ii) as average temperatures across space were similar
174 between gradient and uniform landscapes (27.4°C; SD = 3.85°C and 26.9°C; SD = 1.53°C,
175 respectively), temperatures at the start of gradient landscapes were relatively cooler than in
176 uniform landscapes (24.3°C; SD = 2.6°C and 27.6°C; SD = 1.4°C, respectively). However, we
177 note that our temperature treatment still reflects the presence and absence of a temperature
178 gradient across space in gradient and uniform landscapes, respectively.
179
180 **Range expansion**
181 To initiate range expansion, we established genetically diverse *Lemna* populations, with each
182 population consisting of an even density of 20 accessions ($N$ = 20 individuals per accession for a
183 founding population size of $N$ = 400 individuals). We seeded each population at one end of each
184 landscape, allowing 2 days for plants to acclimate before range expansion. In gradient
185 landscapes, we seeded populations at the cooler end of the landscape and allowed range
186 expansion into increasingly warmer temperatures (Fig. 1a). To allow all populations the
187 opportunity to colonize the full spatial extent of the landscape, the experiment ran for 112 days.
188 During our experiment, we lost one replicate due to structural damage and lost 10 replicates on
189 one bench due to a disturbance event that disrupted population spread. We also lost 6 replicates
190 due to heavy algal growth on the water surface that obstructed population spread. In total, we

retained 33 experimental landscapes across four benches ($N$ = 16 gradient landscapes; $N$ = 17 uniform landscapes).

**Quantifying range expansion speed**

We quantified the mean and variability in range expansion speed across landscapes for the initial 24 days (i.e., ~5–12 generations) of range expansion. This timescale represents population spread during the exponential growth phase and thus is most consistent with theoretical models of range expansion (Kot et al. 1996; Skellam 1951). Also, some populations had reached the range limit of landscapes by day 24. These replicates would not be able to spread further and their inclusion after 24 days would artificially reduce the average and among-replicate variability in range expansion speed (i.e., the ceiling effect).

To quantify range expansion speed, we took aerial photographs of each landscape every 4 days (Nikkon D750; AF-S Nikkor 24-120 mm f/4G ED VR). From these images, we first quantified the maximum distance travelled (cm) for each population by measuring the distance reached by the furthest individual every 4 days. We then quantified the mean and among-replicate variability in the distance travelled at each treatment level and time point. To estimate the difference in among-replicate variability of distance travelled for gradient and uniform landscapes, we calculated the log coefficient of variation ratio (lnCVR; Nakagawa et al. 2015) as:

$$lnCVR = \frac{lnCV_E}{lnCV_C} + \frac{1}{2(n_E-1)} - \frac{1}{2(n_C-1)} \qquad (1)$$

where subscripts $E$ and $C$ refer to the experimental (i.e., gradient) and control (i.e., uniform) landscapes, CV is the coefficient of variation, and $n$ is the sample size. We calculated lnCVR

such that positive values correspond to larger variability in distance travelled among gradient compared to uniform landscapes. We use lnCVR because CV accounts for the linear and positive mean-variance relationship on the log scale (Fig. S2; Taylor 1961). To report differences in CV, we back-transformed estimates of lnCVR.

**Quantifying range-front population density and steepness**

We quantified spatiotemporal changes in population density at the range front by estimating the percent cover of live (i.e., green) fronds on the water surface. We did this by colour thresholding images obtained every 4 days using ImageJ (v1.53) and estimating percent cover in 2 cm x 12.5 cm grids at the range front (defined as the first 12 cm from the furthest travelled individual). We then fit a logistic model of percent cover across space for each landscape to quantify the maximum population density at the range front at each time point. We also quantified the steepness of the range boundary (i.e., the rate of increase in population density) by fitting an exponential model to the first three estimates of percent cover at the range front of each landscape. Steepness was quantified as the exponent obtained from each model (Legault et al. 2020).

**Quantifying range-front evolution**

We quantified evolution as the change in genotype frequencies due to genotype sorting from the founding population. Post-experiment, we haphazardly sampled 12 individual rafts of duckweeds from each replicate range front. Each sample was then genotyped using four microsatellite markers in a single multiplex reaction (Appendix S1; Table S2; Hart et al. 2017). We successfully obtained genotype sequences for 272 individuals (88% of all genotyped samples).

236 To balance the number of samples obtained within each replicate and treatment, we rarefied
237 samples and dropped replicates represented by less than $N = 6$ individuals due to DNA extraction
238 or genotyping failure. For all downstream analyses, we therefore obtained a total of $N = 6$
239 individuals per replicate, for 10 and 17 replicates of gradient and uniform landscapes,
240 respectively. We note a higher extraction and genotyping failure for samples obtained from
241 gradient landscapes possibly due to greater damage to plant tissue from heat stress.
242
243 To investigate whether genotype sorting in the experiment led to consistent trait evolution, we
244 also measured a suite of genotype-specific traits *ex situ* in incubators and across a range of
245 temperatures (Appendix S2; Fig. S1). We parameterized traits hypothesised to be ecologically
246 relevant to range expansion across thermally variable landscapes, including: maximum growth
247 rate ($r_{max}$); thermal optimum ($T_{opt}$); critical thermal maximum ($CT_{max}$); critical thermal minimum
248 ($CT_{min}$); thermal breadth (i.e., the range of temperatures for which growth rate is within 80% of
249 the maximum; Padfield et al. 2021); thermal tolerance (i.e., the difference between $CT_{max}$ and
250 $CT_{min}$); mean specific-leaf area (SLA; $cm^2/g$); mean root-shoot ratio (cm/mg); and plasticity in
251 both SLA and root-shoot ratio, as quantified by its CV across temperature (see Table S10 for
252 trait estimates at the genotype level). Before analyses, we scaled and centred each trait, and
253 estimated mean trait values at the population level for both our founding and evolved populations
254 by weighting trait values by the observed genotype frequencies of each population.
255
256 **Statistical analyses**
257 We tested whether temperature treatment led to differences in the ecological dynamics of range
258 expansion. First, we tested for treatment differences in mean range expansion speed by fitting a

259 linear mixed-effects model using the *lme4* package (Bates et al. 2015). We fit maximum distance
260 travelled (cm) as the response variable and an interaction between time (day) and temperature
261 treatment (gradient *vs* uniform) as fixed predictors, where mean range expansion speed is
262 modelled as slopes (cm/day). We also included bench ID as a fixed covariate and fitted a random
263 slope (i.e., speed) for each replicate. Second, we tested for treatment differences in among-
264 replicate variability of distance travelled by fitting a linear model with lnCVR as the response
265 variable and time as the predictor. We modelled the temporal trend in lnCVR as visual
266 inspections of CV in distance travelled showed changes over time for both gradient and uniform
267 landscapes (Fig. 2b). For sensitivity analyses, we also conducted a linear meta-regression of
268 lnCVR to explicitly model the sampling variation around each observation (Appendix S3). Third,
269 we tested for treatment differences in range-front population density (i.e., carrying capacity) and
270 steepness of the range boundary (i.e., exponent) by fitting separate linear regressions with either
271 population density or steepness as the response variable, respectively, and time, temperature
272 treatment, and their interaction as predictors. For sensitivity analyses, we also conducted a
273 separate meta-regression of population density and steepness by including the standard error
274 around each observation using the package *metafor* (Viechtbauer 2010).
275
276 We also tested whether temperature treatment led to differences in the evolutionary dynamics of
277 range expansion. First, we tested for treatment differences in the amount of genotypic or trait
278 change, as estimated by the Euclidean distance between the initial genotype or trait frequency in
279 the founding population and the post-experimental genotype or trait frequency for each
280 landscape. We fit separate linear regressions with Euclidean distance of genotype or trait
281 frequencies as the response variable, temperature treatment as the predictor, and bench ID as a

282 fixed covariate. Second, we tested for treatment differences in the final genotype or trait
283 composition in range-front populations. Here, we quantified compositional dissimilarity of
284 genotypes or traits across all pairwise populations within each treatment using Euclidean
285 dissimilarity matrices. We then conducted separate PERMANOVAs using *adonis2* in the *vegan*
286 package (Okansen et al. 2022) with genotype or trait dissimilarity among replicates as the
287 response variable, temperature treatment as the predictor, and bench ID as a fixed covariate.
288 Upon observing differences in genotype composition, we tested whether certain genotypes arose
289 to higher frequencies than predicted by chance by conducting a post-hoc binomial test on the
290 mean frequency of each genotype for each temperature treatment. Third, we tested whether
291 temperature treatment led to differences in the amount of among-replicate variability found in
292 the genotype composition of range-front populations. To quantify the amount of observed
293 among-replicate variability, we first averaged genotype frequencies across replicates within each
294 treatment. For each temperature treatment, we then calculated the Euclidean distance between
295 this mean genotype composition and the observed genotype composition of each replicate. As a
296 measure of the observed among-replicate variability in genotype composition, we then summed
297 these Euclidean distances across all replicates within each treatment. We tested for treatment
298 differences in among-replicate variability through a permutation test, with Euclidian distances
299 permuted randomly across treatment 100,000 times. Finally, we tested whether the observed
300 among-replicate variability in each treatment differed from that predicted by random sampling.
301 To quantify among-replicate variability predicted by random sampling, we first pooled
302 genotypes across replicates within each temperature treatment. From this pool, we randomly
303 drew 6 individuals with replacement (i.e., representing the 6 genotypes in our observed data) and
304 repeated this $N$ times for each treatment, where $N$ is the number of replicates for gradient ($N$ =

305 10) and uniform landscapes ($N$ = 17). We then estimated the mean genotype composition for
306 each temperature treatment and calculated the Euclidean distance between the simulated mean
307 genotype composition and the simulated genotype composition of each replicate. We summed
308 these Euclidean distances for each treatment as a measure of the among-replicate variability in
309 genotype composition predicted by random sampling. We repeated this simulation a total of
310 100,000 times to estimate the probability of obtaining the observed among-replicate variability in
311 genotype composition for each treatment based on random sampling. All model-fitting was
312 conducted in R (R Core Team 2020).
313

314 **RESULTS**

315 **Temperature treatment on range expansion speed**

316 On average, we found that range expansion speed across gradient landscapes was slower than
317 across uniform landscapes (time by treatment effect: $P$ = 0.016; Table S4; Fig. 2a), consistent
318 with prediction (ii). Over 24 days of range expansion, the presence of a spatial temperature
319 gradient reduced the average speed of range expansion by 50.9% (95% CI: 36.0% to 53.8%)
320 compared to uniform landscapes (Table S4). We also found that the among-replicate variability
321 in distance travelled differed between gradient and uniform landscapes (Fig. 2b and 2c). At the
322 initial stages of range expansion, we found that there was less among-replicate variability (CV)
323 in distance travelled across gradient compared to uniform landscapes (e.g., a 40.3% [95% CI:
324 28.6% to 56.8%] reduction in CV across gradient compared to uniform landscapes on day 4;
325 Table S5), consistent with prediction (i). However, we found a significant increase in lnCVR
326 over time (lnCVR slope: $P$ = 0.002) such that by day 24, CV in distance travelled was 78.2%
327 (95% CI: 28.6% to 151.0%) greater across gradient than uniform landscapes (Fig. 2c), contrary

328 to prediction. This result was consistent when including sampling variation around lnCVR in the
329 linear model (Table S5).
330
331 **Temperature treatment on range-front density and steepness**
332 We found that the population density reached at the range front differed over time and between
333 gradient and uniform landscapes (Fig. 2d-f). Although range-front densities were initially similar
334 between gradient and uniform landscapes, population density increased more rapidly over time
335 for gradient landscapes (treatment by time effect: $P = 0.002$; Fig. 2f), consistent with prediction
336 (ii). By day 24, population density at the range front was 88.1% (95% CI: 76.5% to 104.0%)
337 higher in gradient compared to uniform landscapes (Table S6). Along with increased population
338 density, we also found range boundaries to be steeper in gradient landscapes (Table S7; Figure
339 S3), consistent with prediction (ii). These results were consistent in sensitivity models that
340 included sampling error in estimates of range-front population density and steepness (Tables S6
341 and S7).
342
343 **Temperature treatment on evolutionary change**
344 We found that evolution in range-front populations (i.e., change in genotype frequencies from
345 the founder population) occurred in both gradient and uniform landscapes (Intercept: $P < 0.001$;
346 Table S8). We found partial support for prediction (iii) that selection is greater in gradient
347 landscapes. On average, the observed among-replicate variability in genotype composition was
348 greater in uniform compared to gradient landscapes (Fig. 4), although permutation tests revealed
349 that this treatment difference was non-significant ($P = 0.304$). Importantly, we found that the
350 observed among-replicate variability in genotype composition was greater than predicted by

351 random sampling for both gradient ($P = 0.003$) and uniform ($P < 0.001$) landscapes (Fig. 4). We
352 also found that genotype composition of range-front populations differed between gradient and
353 uniform landscapes after range expansion (PERMANOVA: $P = 0.002$; Table S9; Fig. 3a).
354 Specifically, range-front populations in gradient landscapes were dominated by the *L. turionifera*
355 genotype (Fig. 3c), with post-hoc binomial tests showing that *L. turionifera* consistently
356 increased in frequency in gradient landscapes ($P < 0.001$) but not in uniform landscapes ($P =$
357 $0.869$), suggesting selection for this genotype in the former (Fig. 3e).
358
359 Trait evolution (i.e., change in trait frequencies from the founder population) occurred in both
360 gradient and uniform landscapes (Intercept: $P = 0.004$; Table S8; Fig. S4). However, contrary to
361 prediction (iv), out of the 11 traits assessed we did not find significant treatment differences in
362 the extent of trait change (Treatment effect: $P = 0.345$; Table S8) or in trait composition of
363 range-front populations (PERMANOVA: $P = 0.088$; Table S9; Fig. S4).
364
365 **DISCUSSION**
366 Recent studies have highlighted that rapid evolution can complicate our ability to predict the eco-
367 evolutionary dynamics of range expansions (Miller et al. 2020; Shaw et al. 2023; Williams et al.
368 2019; Zilio et al. 2023). Here, we used replicate range-expanding populations to empirically test
369 whether the presence of selection from an abiotic gradient across landscapes could modify the
370 among-replicate variability, and hence predictability, of range expansion speed. Notably, we
371 found that over time range expansion speed became more variable, and hence less predictable, in
372 landscapes with a spatial temperature gradient than without (Fig. 2c). This occurred despite
373 gradient landscapes having slower range expansions on average, greater range-front population

374 densities (Fig. 2), and genetic signatures consistent with increased selection (Fig. 3)– conditions
375 that would otherwise predict less gene surfing and thus more consistency in the speed of range
376 expansions across replicate populations (Miller et al. 2020; Phillips 2015; Williams et al. 2019).
377 Our results therefore challenge current theory and highlight the complexities of predicting range
378 expansions even in highly standardised, replicate mesocosms with simple environmental
379 variation.
380
381 We found that the greater variability in range expansion speed observed for gradient compared to
382 uniform landscapes over time is driven by a combination of rapidly decreasing among-replicate
383 variability (CV) in distance travelled for uniform landscapes, and slightly increasing CV for
384 gradient landscapes over time (Fig. 2b). In uniform landscapes, the decrease in CV of distance
385 travelled over time occurred as mean range expansion speed increased more quickly than the
386 variance observed across replicates (Fig. 2a). A rapid increase in mean range expansion speed
387 across uniform landscapes is consistent with previous experimental evolution work on range
388 expansions, which found that range expansion speed can increase under constant environments
389 due to spatial sorting for dispersal phenotypes and low-density selection for increased
390 reproductive output at the range front (Ochocki & Miller 2017; Wagner et al. 2017; Weiss-
391 Lehman et al. 2017). In contrast, for gradient landscapes, the slight increase in CV of distance
392 travelled over time occurred as the variance in speed among replicates increased more quickly
393 than the mean range expansion speed (Fig. 2a). This occurred as range expansion remained slow
394 for most gradient landscapes but rapidly sped up in a few replicates (Fig. 2a), consequently
395 elevating the among-replicate variability observed over time.
396

397 It is possible that the faster range expansion seen in some of these gradient landscapes was partly
398 driven by selection from the temperature gradient (Moerman et al. 2022; Phillips et al. 2006;
399 Szücs et al 2017; Williams et al. 2016). We found that genotype composition in gradient
400 landscapes had consistently higher frequencies of *L. turionifera* genotypes at the range front
401 (Fig. 3c and 3d). In contrast, *L. turionifera* did not achieve frequencies >0.5 in any range-front
402 population for uniform landscapes (Fig. S5). We note that the evolutionary dynamics described
403 above reflect longer term range expansion and selection after 112 days (~22-56 generations),
404 while the population dynamics reflect shorter term range expansion in the first 24 days (~4-12
405 generations). Even so, comparison to genetic data obtained at an earlier point in time from the
406 fastest range-expanding replicates confirm that *L. turionifera* had reached high frequencies at the
407 range-front of gradient landscapes but not in uniform landscapes (Fig. S6), suggesting that rapid
408 evolution in the former occurred as early as within the first 36 days (i.e., 7–18 generations) of
409 range expansion.
410
411 While we did not find trait composition to differ significantly between gradient and uniform
412 landscapes within the 11-dimensional trait space (Fig. S4), post-hoc comparison of univariate
413 trait means revealed that *L. turionifera* has both the highest mean estimate of thermal breadth and
414 the lowest maximum growth rates among all genotypes (Table S10). The importance of
415 maintaining performance across a broader range of temperatures through thermal breadth
416 evolution has been long emphasised in studies of range expansion across latitudinal gradients in
417 climate (Ackerly 2003; Lancaster 2016; Lancaster 2022) and is also consistent with studies that
418 report a positive relationship between range size and niche breadth (Slatyer et al. 2013). While it
419 could be surprising that range-expanding populations are also fixed for the genotype with the

420 lowest maximum growth rate, this could be explained by generalist-specialist trade-offs between
421 sustaining growth rates across a wider range of temperatures and obtaining high growth rates at
422 the temperature optimum (Huey & Hertz 1984). Additionally, models of range expansion that
423 incorporate density-dependence and life-history trade-offs also predict that higher population
424 densities and steeper range boundaries, as observed in our gradient landscapes, can favour *K*-
425 selected traits (e.g., increased competitive ability) at the range front even if this comes at a cost
426 of *r*-selected traits (e.g., increased reproductive output and growth rates; Burton et al. 2010;
427 Pachepsky & Levine 2011; Williams et al. 2016).
428
429 However, while the consistently high frequency of *L. turionifera* genotypes suggest that selection
430 was stronger at the range front of gradient over uniform landscapes, we also found in both
431 landscapes that the among-replicate variability in genetic composition was greater than predicted
432 by random sampling (Fig. 4). Such a pattern could result if the eco-evolutionary dynamics of
433 range expansion in landscapes with environmental variation is governed by a combination of
434 selection and spatial priority effects, such that the genotypes available to respond to selection in
435 range-front populations is shaped by individuals that initially occupy the range front through
436 chance dispersal (Baym et al. 2016; Hallatschek et al. 2007; Hewitt 2000; Williams et al. 2016).
437 Taken together, we propose that spatial priority effects and its variance-generating effects at the
438 range front, combined with directional selection from abiotic gradients in space, could lead on
439 average to slower but more variable speeds during range expansion, relative to range expansion
440 across uniform environments.
441

Our results highlight that even in ecological conditions under which the effects of gene surfing are reduced, the speed of range expansion can be variable and difficult to predict. Previous experimental and theoretical work suggest the predictability of range expansion speed depends on the balance of evolutionary processes that generate and reduce variability (i.e., gene surfing and selection, respectively) and the ecological factors that tip this balance (Miller et al. 2020; Williams et al. 2019). We additionally suggest that predicting the dynamics of range expansion may require an understanding of how selection interacts with spatial priority effects, and whether priority effects could hamper the response to selection and increase among-replicate variability in the speed of range expansion. As populations traverse across environmentally variable and complex landscapes, studies of natural range expansions will need to incorporate how selection from underlying environmental variation in space can influence our ability to predict future range expansions.

## ACKNOWLEDGEMENTS

We thank H. Ahmed, M. Catalani, A. Doherty, K. Kubeck, E. Menchions, T. Scriber, and P. Seppala for their help with plant and greenhouse maintenance, and for providing assistance with experimental setup. We thank D. Moxley and A. Wong for their assistance with genetic work. We are grateful to R. Germain, S. Otto, M. Tseng, and J. Williams for their comments on earlier versions of the manuscript. This work was supported by the UBC International Doctoral Fellowship and the SSE Greg Lewontin Award to TU, and a Discovery Grant from the Natural Sciences and Engineering Research Council of Canada to ALA.

## REFERENCES

Ackerly, D.D. (2003). Community assembly, niche conservatism, and adaptive evolution in changing environments. *Int. J. Plant Sci.*, 164, S165–S184.

Appenroth, K.J., Teller, S. & Horn, M. (1996). Photophysiology of turion formation and germination in *Spirodela polyrhiza*. *Biol. Plantarum*, 38, 343–351.

Bates, D., Mächler, M., Bolker, B. & Walker, S. (2015). Fitting linear mixed-effects models using lme4. *J. Stat. Softw.*, 67, 1–48.

Baym, M., Lieberman T.D., Kelsic, E.D., Remy, C., Gross, R., Yelin, I. & Kishony, R. (2016). Spatiotemporal microbial evolution on antibiotic landscapes. *Science*, 353, 1147–1151.

Braglia, L., Breviario, D., Gianì, S., Gavazzi, F., De Gregori, J. & Morello, L. (2021a). New insights into interspecific hybridization in *Lemna* L. Sect. *Lemna* (Lemnaceae Martinov). *Plants*, 10, 2767.

Braglia, L., Lauria, M., Appenroth, K.J., Bog, M., Breviario, D., Grasso, A., *et al*. (2021b). Duckweed species genotyping and interspecific hybrid discovery by Tubulin-Based Polymorphism Fingerprinting. *Front. Plant. Sci.*, 12, 625670.

Burton, O.J., Phillips, B.L. & Travis, J.M.J. (2010). Trade-offs and the evolution of life-histories during range expansion: Evolution during range expansion. *Ecol. Lett.*, 13, 1210–1220.

Chen, I.C., Hill, J.K., Ohlemüller, R., Roy, D.B. & Thomas, C.D. (2011). Rapid range shifts of species associated with high levels of climate warming. *Science*, 333, 1024–1026.

Chuang, A. & Peterson, C.R. (2016). Expanding population edges: Theories, traits, and trade-offs. *Glob. Change Biol.*, 22, 494–512.

Docauer, D. M. (1983). *A nutrient basis for the distribution of the Lemnaceae*. Dissertation. University of Michigan, Ann Arbor, Michigan, USA.

Excoffier, L., Foll, M. & Petit, R.J. (2009). Genetic consequences of range expansions. *Annu. Rev. Ecol. Evol. S.*, 40, 481–501.

Freedman, M.G., Dingle, H., Strauss, S.Y., & Ramírez, S.R. (2020). Two centuries of monarch butterfly collections reveal contrasting effects of range expansion and migration loss on wing traits. *Proc. Natl. Acad. Sci. U.S.A.*, 117, 28887–28893.

Fronhofer, E.A., Nitsche, N. & Altermatt, F. (2017). Information use shapes the dynamics of range expansions into environmental gradients. *Glob. Ecol. Biogeogr.,* 26, 400–411.

Gilbert, K.J., Sharp, N.P., Angert, A.L., Conte, G.L., Draghi, J.A., Guillaume, F., *et al.* (2017). Local adaptation interacts with expansion load during range expansion: Maladaptation reduces expansion load. *Am. Nat.*, 189, 368–380.

Hallatschek, O., Hersen, P., Ramanathan, S. & Nelson, D.R. (2007). Genetic drift at expanding frontiers promotes gene segregation. *Proc. Natl., Acad. Sci. U.S.A.*, 104, 19926–19930.

Hart, S.P., Turcotte, M.M. & Levine, J.M. (2019). Effects of rapid evolution on species coexistence. *Proc. Natl., Acad. Sci. U.S.A.*, 116, 2112–2117.

Hewitt, G. (2000). The genetic legacy of the Quaternary ice ages. *Nature*, 405, 907–913.

Huey, R.B. & Hertz, P.E. (1984). Is a Jack-of-All-Temperatures a Master of None? *Evol.,* 38, 441–444.

Iseli, E., Chisholm, C., Lenoir, J., Haider, S., Seipel, T., Barros, A., *et al.* (2023). Rapid upwards spread of non-native plants in mountains across continents. *Nat. Ecol. Evol.*, 7, 405–413.

Klopfstein, S., Currat, M. & Excoffier, L. (2006). The fate of mutations surfing on the wave of a range expansion. *Mol. Biol. Evol.*, 23, 482–490.

Kot, M., Lewis, M.A. & Van Den Driessche, P. (1996). Dispersal data and the spread of invading organisms. *Ecol.*, 77, 2027–2042.

Lancaster, L.T., Dudaniec, R.Y., Hansson, B. & Svensson, E.I. (2015). Latitudinal shift in thermal niche breadth results from thermal release during a climate-mediated range expansion. *J. Biogeogr.*, 42, 1953–1963.

Lancaster, L.T. (2016). Widespread range expansions shape latitudinal variation in insect thermal limits. *Nat. Clim. Change*, 6, 618–621.

Lancaster, L.T. (2022). On the macroecological significance of eco-evolutionary dynamics: The range shift–niche breadth hypothesis. *Philos. T. R. Soc. B.*, 377, 20210013.

Landolt, E. (1986). *Biosystematic investigations in the family of duckweeds, Lemnaceae: the family of Lemnaceae, a monographic study*. Volume 2: Morphology, karyology, ecology, geographic distribution, systematic position, nomenclature descriptions. Veroeffentlichungen des Geobotanischen Institutes der ETH, Stiftung Rubel, Zurich, Switzerland.

Larsen, C.D. & Hargreaves, A.L. (2020). Miniaturizing landscapes to understand species distributions. *Ecography*, 43, 1625–1638.

Legault, G., Bitters, M.E., Hastings, A. & Melbourne, B.A. (2020). Interspecific competition slows range expansion and shapes range boundaries. *Proc. Natl. Acad. Sci. U.S.A.*, 117, 26854–26860.

Lustenhouwer, N., Moerman, F., Altermatt, F., Bassar, R.D., Bocedi, G., Bonte, D., *et al.* (2023). Experimental evolution of dispersal: Unifying theory, experiments and natural systems. *J. Anim. Ecol.*, 92, 1113–1123.

Miller, T.E.X., Angert, A.L., Brown, C.D., Lee-Yaw, J.A., Lewis, M., Lutscher, F., *et al.* (2020). Eco-evolutionary dynamics of range expansion. *Ecol.*, 101. e03139.

Moerman, F., Fronhofer, E.A., Altermatt, F. & Wagner, A. (2022). Selection on growth rate and local adaptation drive genomic adaptation during experimental range expansions in the protist *Tetrahymena thermophila*. *J. Anim. Ecol.*, 91, 1088–1103.

Nadeau, C.P. & Urban, M.C. (2019). Eco-evolution on the edge during climate change. *Ecography*, ecog.04404.

Nakagawa, S., Poulin, R., Mengersen, K., Reinhold, K., Engqvist, L., Lagisz, M., *et al.* (2015). Meta-analysis of variation: Ecological and evolutionary applications and beyond. *Methods Ecol. Evol.*, 6, 143–152.

Ochocki, B.M. & Miller, T.E.X. (2017). Rapid evolution of dispersal ability makes biological invasions faster and more variable. *Nat. Commun.*, 8, 14315.

Oksanen, J., Simpson, G.L., Blanchet, F.G., Kindt, R., Legendre, P. & Minchin, P.R. (2022). Vegan: Community ecology package (v 2.6–2).

Pachepsky, E. & Levine, J.M. (2011). Density dependence slows invader spread in fragmented landscapes. *Am. Nat.*, 177, 18–28.

Padfield, D., O'Sullivan, H. & Pawar, S. (2021). rTPC and nls.multstart: A new pipeline to fit thermal performance curves in R. *Methods Ecol. Evol.*, 12, 1138–1143.

Perrier, A., Sánchez-Castro, D. & Willi, Y. (2020). Expressed mutational load increases toward the edge of a species' geographic range. *Evol.*, 74, 1711–1723.

Phillips, B.L. (2015). Evolutionary processes make invasion speed difficult to predict. *Biol. Invasions*, 17, 1949–1960.

Phillips, B.L., Brown, G.P., Webb, J.K. & Shine, R. (2006). Invasion and the evolution of speed in toads. *Nature*, 439, 803–803.

R Core Team (2020). *R: A language and environment for statistical computing*. R Foundation for Statistical Computing, Vienna, Austria.

Shaw, A.K., Lutscher, F. & Popovic, L. (2023). Pushed to the edge: Spatial sorting can slow down invasions. *Ecol. Lett.*, 26, 1293–1300.

Skellam, J.G. (1951). Random Dispersal in Theoretical Populations. *Biometrika*, 38, 196–218.

Slatyer, R.A., Hirst, M. & Sexton, J.P. (2013). Niche breadth predicts geographical range size: A general ecological pattern. *Ecol. Lett.*, 16, 1104–1114.

Szűcs, M., Vahsen, M.L., Melbourne, B.A., Hoover, C., Weiss-Lehman, C. & Hufbauer, R.A. (2017). Rapid adaptive evolution in novel environments acts as an architect of population range expansion. *Proc. Natl. Acad. Sci. U.S.A.*, 114, 13501–13506.

Urquhart-Cronish, M., Angert, A.L., Otto, S.P. & MacPherson, A. (2022). Density-dependent selection during range expansion affects expansion load in life-history traits. *bioRxiv*, 2022.11.08.515702.

Viechtbauer, W. (2010). Conducting meta-analyses in R with the metafor package. *J. Stat. Softw.*, 3, 1–48.

Volkova, P.A., Nachatoi, V.A. & Bobrov, A.A. (2023). Hybrid between *Lemna minor* and *L. turionifera* (*L.* × *japonica*, Lemnaceae) in East Europe is more frequent than parental species and poorly distinguishable from them. *Aquat. Bot.*, 184, 103593.

Wagner, N.K., Ochocki, B.M., Crawford, K.M., Compagnoni, A. & Miller, T.E.X. (2017). Genetic mixture of multiple source populations accelerates invasive range expansion. *J. Anim. Ecol.*, 86, 21–34.

Weiss-Lehman, C., Hufbauer, R.A. & Melbourne, B.A. (2017). Rapid trait evolution drives increased speed and variance in experimental range expansions. *Nat. Commun.*, 8, 14303.

Williams, J.L., Kendall, B.E. & Levine, J.M. (2016). Rapid evolution accelerates plant population spread in fragmented experimental landscapes. *Science*, 353, 482–485.

Williams, J.L., Hufbauer, R.A. & Miller, T.E.X. (2019). How evolution modifies the variability of range expansion. *Trends Ecol. Evol.*, 34, 903–913.

Zilio, G., Krenek, S., Gougat-Barbera, C., Fronhofer, E.A. & Kaltz, O. (2023). Predicting evolution in experimental range expansions of an aquatic model system. *Evol. Lett.*, 7, 121–131.

**Figures**

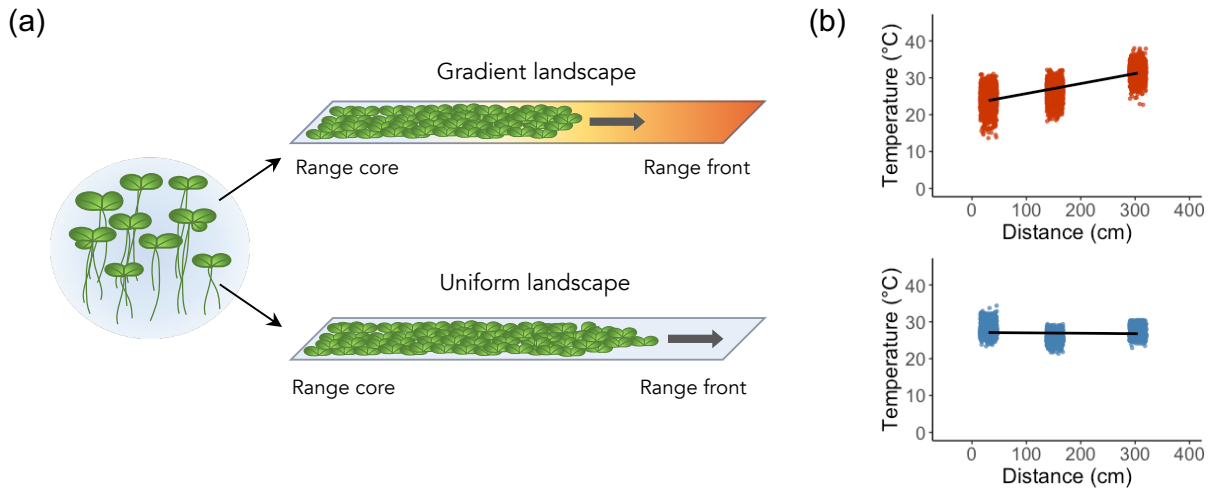


Figure 1. Experimental range expansion across landscapes with and without a spatial gradient in temperature. (a) Replicate, mixed-genotype populations of *Lemna* expand their experimental ranges across increasingly warmer temperatures (blue to red) from the range core to the range front in gradient landscapes, or across benign and constant temperatures in uniform landscapes. (b) Observed temperatures across gradient (red) and uniform (blue) landscapes during the experiment. Lines represent the slopes of linear models of temperature by distance. We found a significant and positive temperature slope in gradient landscapes ($\beta_{gradient}$ = 0.027, 95% CI: 0.027 to 0.028 °C/cm; $t$ = 126.49; $P$ < 0.001) and a slightly negative slope in uniform landscapes ($\beta_{uniform}$ = –0.001, 95% CI: –0.002 to 0.000 °C/cm; t = 68.50; $P$ < 0.01).

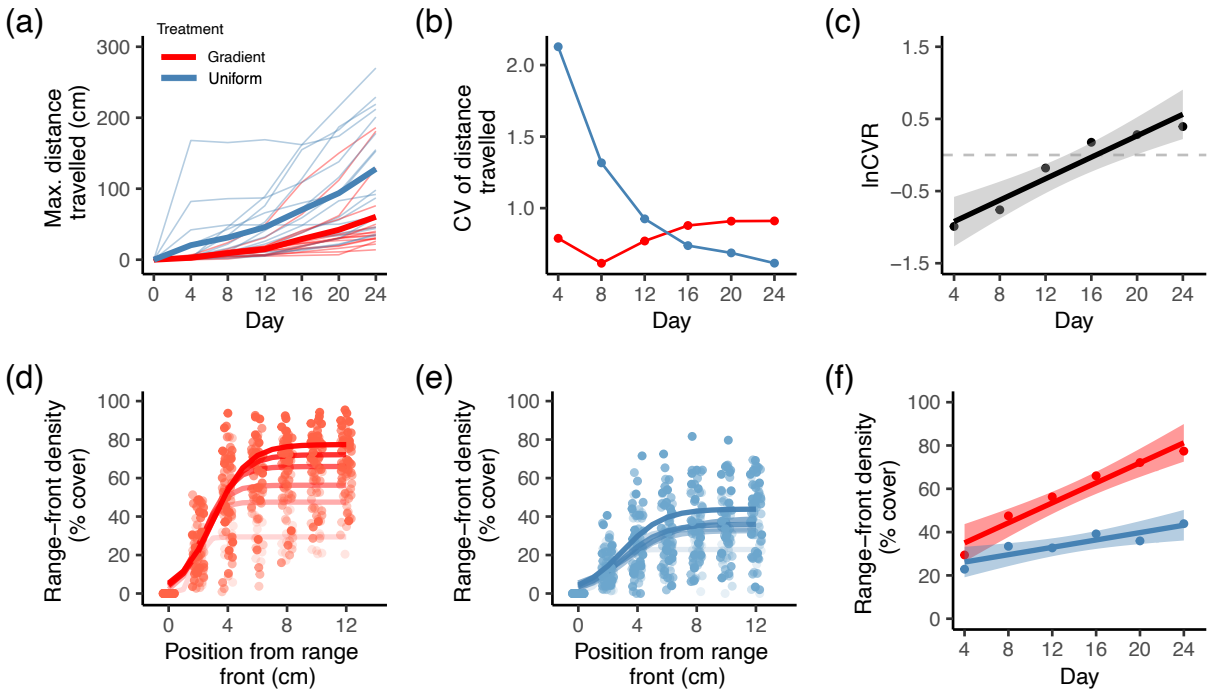


Figure 2. Population dynamics of range expansion across landscapes with (red) and without (blue) a temperature gradient across space. (a) Each line represents the maximum distance travelled over time for a single, replicate range expansion (mean values shown by thick lines). (b) Among-replicate variability (CV) in distance travelled over time for gradient and uniform landscapes. (c) Slope and 95% CI of changes in the log coefficient of variation ratio (lnCVR) over time, where estimates of lnCVR below zero (dashed grey line) indicate that there is less among-replicate variability (CV) across gradient than uniform landscapes. (d-e) Population densities at the range front (i.e., the first 0 to 12 cm) during range expansion. Lines show model predictions from a logistic regression of density across space, with increasing colour intensity representing changes over time from day 4 to 24. (f) Slope and 95% CI obtained from a linear regression of range-front density over time.

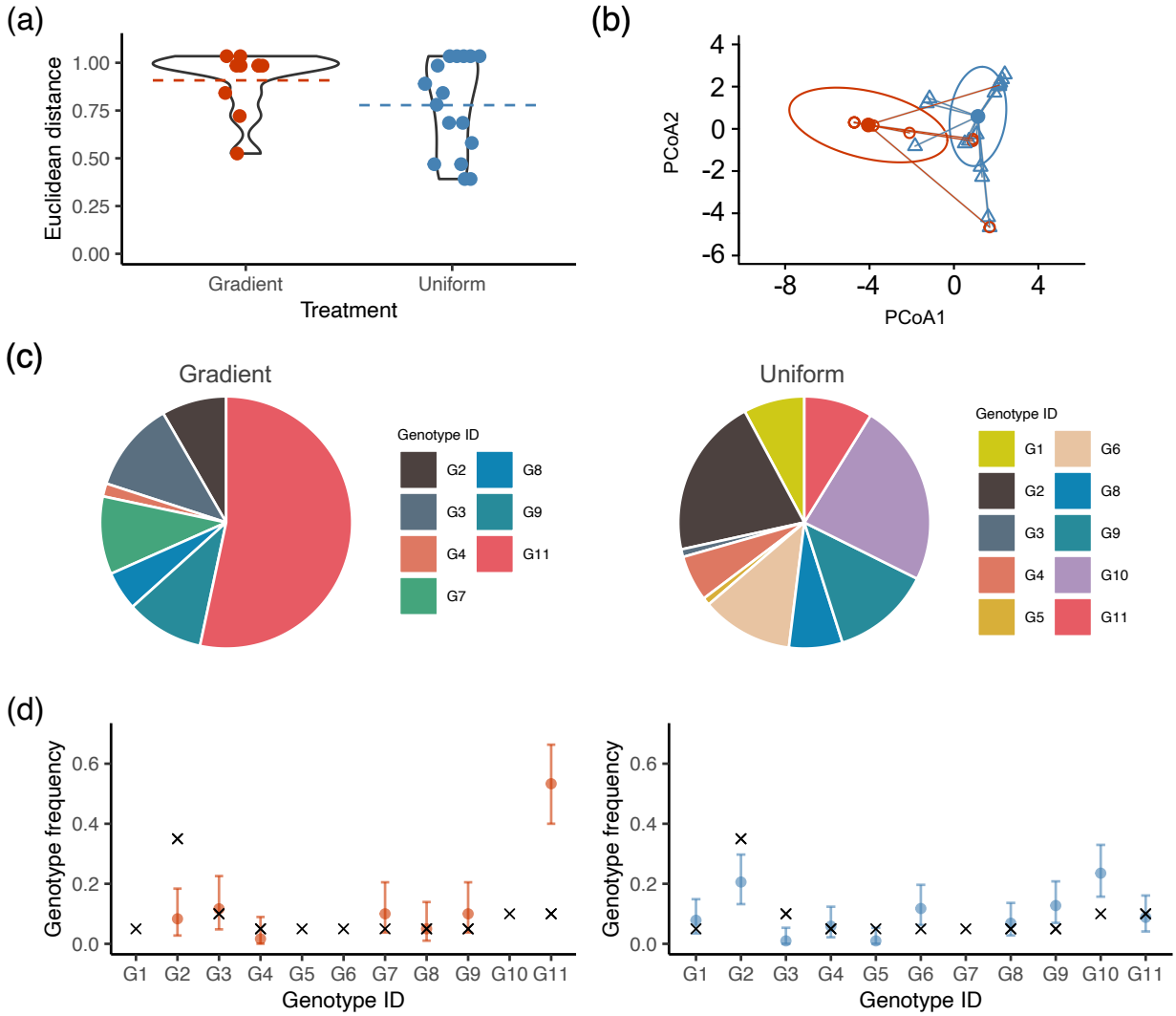


Figure 3. Evolutionary dynamics of range expansion across landscapes with and without a temperature gradient across space. (a) Violin plot for the magnitude of evolution observed in gradient (red) and uniform (blue) landscapes, as quantified as the Euclidean distance of genotype frequencies between founder and evolved populations at the range front. Points show the amount of change in genotype frequencies for each replicate, while dashed lines represent the mean change. (b) Genotype composition of range-front populations in gradient (red) and uniform (blue) landscapes. The first two axes of a Principal Coordinates Analysis (PCoA) are shown, accounting for 43.7% of the total variation in genotype composition. Filled circles are treatment

637 centroids, while clear symbols are replicate populations in each treatment. Ellipses represent one
638 standard deviation around treatment centroids, and lines represent distance from the centroid to
639 each replicate population. (c) Mean genotype frequencies observed across range-front
640 populations in gradient (left) and uniform (right) landscapes, with different colours representing
641 unique genotypes. (d) Genotype frequency for gradient (left) and uniform (right) landscapes.
642 Coloured points and error bars represent observed genotype frequencies and their 95% CIs in
643 evolved range-front populations. The initial genotype frequency in the founder population is
644 denoted by 'x'. G11 represents the cryptic *L. turionifera* genotype.
645
646
647
648
649
650
651
652
653
654
655
656
657
658
659

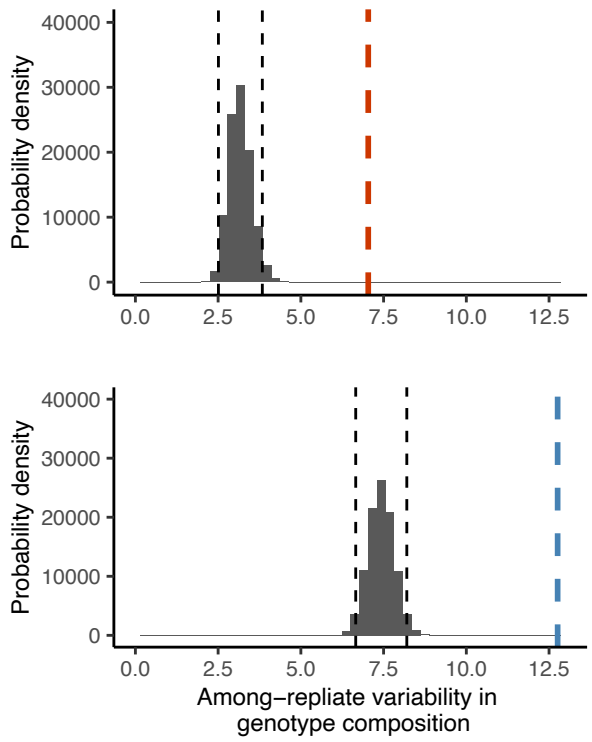


Figure 4. Observed versus simulated among-replicate variability in range-front genotype composition in gradient (top) and uniform (bottom) landscapes. Histograms represent the predicted probability distribution of among-replicate variability in genotype composition due to random sampling alone, with black dotted lines representing the 95% confidence interval. Vertical dashed red and blue lines represent the mean observed among-replicate variability in genotype composition for gradient and uniform landscapes, respectively. Among-replicate variability in genotype composition was quantified as the summed Euclidean distance between the genotypic composition of each replicate population and the mean genotypic composition of each treatment.